Received: 14 April 2022 | Revised: 8 January 2023 | Accepted: 30 January 2023

DOI: 10.1002/jbm.b.35233

RESEARCH ARTICLE

Society For Biomaterials | WILEY

The effect of alginate scaffolds on bone healing in defects formed with drilling model in rat femur diaphysis

Arslan Kagan Arslan[1] | Ali Aydoğdu[2] | Tolga Tolunay[3] | Çağdaş Basat[4] | Resul Bircan[3] | Murat Demirbilek[5]

[1]Department of Orthopedics and Traumatology, Yıldırım Beyazıt University, Yenimahalle Education and Research Hospital, Ankara, Turkey

[2]Faculty of Medicine, Hitit University, Çorum, Turkey

[3]Faculty of Medicine, Department of Orthopedics and Traumatology, Gazi University, Ankara, Turkey

[4]Faculty of Medicine, Department of Orthopedics and Traumatology, Ahi Evran University, Kırşehir, Turkey

[5]Biology Department, Ankara Hacı Bayram Veli University, Ankara, Turkey

Correspondence
Arslan Kagan Arslan, Department of Orthopedics and Traumatology, Yıldırım Beyazıt University, Yenimahalle Education and Research Hospital, Ankara, Turkey.
Email: arslankagan2020@gmail.com

Abstract

Alginate (ALG) is a biocompatible and biodegradable polymer. Mechanical weakness is one of the main problems for the alginate-based scaffolds. Various plasticizer additives or modifications tested to improve the mechanical properties. In the presented study, ALG plasticized with triacetin (TA), and tributyl citrate (TBC) than tested on bone healing. In the presented study, the alginate modified with triacetin or tributyl citrate. In-vitro, and in-vivo efficiency of the scaffolds tested on bone tissue regeneration. Scaffolds fabricated by solvent casting, and physicochemical characterizations performed. Monocytes (THP-1) cultured with scaffolds, and macrophage-released cytokines was determined. In-vivo efficacy of the scaffolds was tested in the rat drill hole model. Alginate and tributyl citrate-modified scaffolds have no cytotoxic effect on osteoblastic cells (MC-3T3). Tributyl citrate modification increased tumor necrosis factor-alpha (TNF-alpha) level but did not increase interleukin -1 beta (IL-1 beta) level. In vivo studies showed that osteoblastic growth was significant in alginate and triacetin-modified scaffolds. However, the best values for osteoclastic activity and osteoid tissue formation seen in the triacetin modification. The results demonstrated that the modified alginate scaffolds were more successful than non-modified alginate scaffolds and can used as long-term bone repairing treatments.

KEYWORDS
bone healing, cytokine levels, hydrophobic plasticizer, rat drill model

1 | INTRODUCTION

In treating orthopedic disorders, biodegradable scaffolds investigated for years. The scaffold, as a matrix, is expected to be non-immunogenic, degradable, and non-toxic. During healing, scaffolds should allow angiogenesis and osteoblastic activity.

Alginate (ALG) is a natural mucopolysaccharide with biocompatible and biodegradable properties. Mechanical weakness is one of the main problems for alginate-based scaffolds. To improve the mechanical properties, various plasticizer additives or modifications are being tested. For instance, Connelly et al. modified alginate with arginine-glycine-aspartic acid sequence.[1] Fructose, glycerol, sorbitol, polyethylene glycol,[2] pectin,[3] and thermoplastic starch/glycerin[4] were studied as a plasticizer to increase mechanical features. Along with plasticizers, the crosslinking procedure affects the mechanical and physicochemical properties of scaffolds. Alginate can be crosslinked physically (ionic bound) with divalent metal ions, such as calcium, and borax. In the presented study, to ensure the stability of the scaffolds, alginate sponges were crosslinked chemically (covalent bound) and used epichlorohydrin.[5]

TA and TBC are derived from citric acid. Citric acid derivatives are used in many areas as a plasticizer, such as cosmetics, food, medical

plastics,[6] and pharmacology.[7] Singh et al. used triethyl citrate to plasticize polylactic acid (PLA).[8] Also, Ljungberg et al. used TA and TBC to plasticize PLA film.[9] TA was studied as a food additive for dogs and determined no toxic effect.[10] In cosmetics, it was determined that concentrations range from 0.8% to 4.0% of TA safe.[11] Segel et al. expressed that 4.5 g/kg/day TA is safe for Canavan disease.[12] Thus, in the present study, % 5 (v/v) TA and TB were used as a plasticizer and investigated the functionality of the alginate-based scaffolds for bone tissue engineering.

In general, after the implantation of a biomaterial into a tissue, it can surround by a large number of macrophages. This may fail implant and, biomaterial-based inflammation. Macrophages are one of the main humoral immune system cells and can release various pro-inflammatory (M1 phenotype) and also anti-inflammatory (M2 phenotype) cytokines and rule the inflation route by releasing cytokines. Cytokines are peptides and have immunoregulatory effects. Pro-inflammatory cytokines (IL-1, TNF-alpha) promote inflation and anti-inflammatory cytokines (IL-4, IL-5, IL-10) suppress inflation.[13] Osteoclasts are bone-resorbing cells. It demonstrated that while some cytokines (IL-1, IL-6, IL-8, and TNF-alpha) up-regulate, the others (IL-3, IL-4, IL-10, IL-12, IL-18) down-regulate the formation of osteoclast cells.[14] Also, some reports indicated that TNF alpha induces osteogenic activities,[15] and promotes bone formation.[16]

The presented study examined the effect of TBC and TA as plasticizers on bone healing. Hence, alginate spongious scaffolds containing TBC, and TA were fabricated. The physicochemical characterizations of the scaffolds were performed. The effects of cytokine-release macrophages interacted with the scaffolds were determined. In in-vivo studies, the scaffolds were evaluated in terms of bone healing, angiogenesis, and osteoblastic activity by histologic studies.

2 | MATERIAL & METHOD

ALG, TBC, TA, nanohydroxyapatite (n-HA), and phorbol-12-myristate-13-acetate (PMA) were purchased from Sigma-Aldrich Company (USA). Cell culture media, fetal calf serum (FCS), Trypsin- Ethylenediaminetetraacetic acid (Trypsin–EDTA), flasks, and plates purchased from Gibco Company (USA). 3-[4,5-dimethylthiazol-2-yl]-2,5-diphenyltetrazolium bromide (MTT), dimethyl sulfoxide (DMSO) obtained from Across Organics (USA). All reagents were analytical grades. In the presented study, ALG was used as the main matrix. TBC and TA were used as the plasticizer. n-HA was used for osteointegration and PMA was used for differentiation of THP-1 cells to macrophages. MTT salt was used to determine the cytotoxicity of the scaffolds. FCS, Trypsin–EDTA, and cell culture medium were used for the cultivation of the cells.

2.1 | Fabrication of scaffolds

The scaffolds were fabricated by the solvent casting method.[17] TBC and TA (5%, v/v) was added to alginate solution (2%, w/v, in distilled water), then nHA (50% w/v) was added to the solutions. The final solutions were poured into a pre-cooled Teflon mold. Each well of the Teflon mold is 5 mm in diameter and 6 mm long. Thus, cylindrical, 5 mm diameter, and 6 mm length scaffolds were fabricated. Same dimension scaffolds were used in all in-vitro and in-vivo tests. For the mechanic test, circular, 10 cm diameter, and 5 mm thickness of Teflon plate mold was used. The molds were frozen overnight at −80°C and lyophilized at −80°C under 0.1 mBar for 24 h.[18] After lyophilization, the scaffolds cross-linked with epichlorohydrin at 70°C for 24 h.[19] The scaffolds were washed with PBS several times. Finally, Alginate-nanohydroxyapatite (Alg-nHA), alginate-triacetin-nanohydroxyapatite (Alg-TA-nHA), alginate- tributyl citrate-nanohydroxyapatite (Alg-TBC-nHA) scaffolds obtained.

2.2 | Characterization of Scaffolds

Morphological analysis of the scaffolds was determined by scanning electron microscopy (SEM, GAIA3 Tescan, Brno Czech Rep.) photographs. Before SEM analysis, scaffolds were coated with gold–palladium with 8 nm thickness.

The swelling and degradation rate of the scaffolds were determined by gravimetric analysis ($n = 8$). The dry form of the scaffolds was weighted. For dehydration, the scaffolds were soaked into 5 mL PBS buffer and incubated for 1 h at 37°C. The wet form of the scaffolds was weighed and recorded. Then, the scaffolds were incubated at 37°C. Once a week, the wet form of the scaffolds was weighed and recorded for 3 weeks.

Chemical characterization of the scaffolds performed by infrared spectra (Fourier transform infrared spectroscopy – attenuated total reflectance (ATR-FTIR), Nicolet™ IS™ 50 spectrometer, Thermo Fisher Scientific, USA). The scans were performed between 600–4000 cm^{-1}, and the resolution was 4 cm^{-1}.

The thermal properties of the scaffolds were analyzed using a thermogravimetric analyzer under a nitrogen atmosphere (Shimadzu Difference Thermogravimetry-60, Perkin Elmer Pyris). The heating rate was 10°C and the range of 25–300°C. An empty platinum pan was used as a reference.

The tensile strength of scaffolds was measured in cells with a 10 N load in room conditions using a mechanical test analyzer (Zwick/Z010). The crosshead speed was set to 10 mm/min. 10 mm width, 10 cm long strips shape scaffolds ($n = 6$) used in mechanical tests.

2.3 | Cell culture studies

Cytotoxicity of the scaffolds ($n = 8$) was evaluated using MC-3T3 cells and results were presented as cell viability (%).[20] The effects of pro-inflammatory cytokine levels of the scaffolds ($n = 6$) on human acute monocyte cell line (THP-1) cells were investigated. Murine calvaria (MC-3T3) cells were cultured in Alpha-Minimum Essential Medium (alpha-MEM), containing 10% FCS, and THP-1 cells were cultured in Roswell Park Memorial Institute-1640 (RPMI-1640) medium,

containing % 15 FCS. The cells were incubated at 37°C, in a 5% carbon dioxide atmosphere.

MC-3T3 cells were seeded into 24 well plates at 10,000 cell/ml concentration. The plates were incubated overnight. Then, scaffolds were placed into the wells. After 24 h incubation, the MTT test was performed. A fresh medium was used as a negative control, medium containing 10% DMSO was used as a positive control.

THP-1 cells were pipetted into 24 well plates at 1×10^6 cell/well concentration. For differentiation of THP-1 cells to macrophages, 3 µL of PMA (200 nM) was pipetted to the wells. The plate was incubated for 3 days. Scaffolds were placed into the wells. After 2 days, media were collected and IL-1 beta and TNF-alpha levels were measured by using commercial kits (Abcam, USA). Non-treated macrophage cells were used as a control.[21]

2.4 | Operations

In-vivo efficiency of the scaffolds in the drill defect model was investigated by using histological assessment. The operations and animal care were reviewed and approved by Kırıkkale University Animal Research Ethics Committee with protocol number 14/06 07.08.2014. Sprague–Dawley rats, 6-week-old with an average weight of 200–300 g, were used. The rats were divided into four groups ($n = 8$) control, Alg-nHA, Alg-TBC-nHA, and Alg-TA-nHA. All operating procedures were undertaken in sterile conditions. Rats were anesthetized by intraperitoneal administration of ketamine hydrochloride (100 mg/kg) and xylazine (5 mg/kg). The surgical site was wiped with povidone-iodide. The midpoint at the rat's thigh between the greater trochanter and distal surface of the lateral condole was determined. Following a small incision from lateral and through extensor and flexor muscle groups, the bone was reached, and approximately 5 mm of periosteum was stripped from the bone surface. The defect was formed using a 2 mm diameter Kirschner wire attached to a low-speed perforator.[22] The defect passed from both cortices and the center of the medullary cavity while being perpendicular to the long axis of the bone. Each scaffold with a 5 mm diameter was implanted in these defects. The wound was closed with non-absorbable sutures. It was observed that the rats tolerated the operation well and were able to regain their normal activities. None of the rats had an infection at the site of the defect. After the operations, rats were sacrificed for 3rd weeks to examine the early healing and inflammation. It was sacrificed at 8th weeks for the late period. The lethal dose of ether anesthesia was used. The femurs of rats were dissected from all surrounding soft tissues except the periosteum for analysis.[23]

In histological assessment, the criteria were presented in Table 1. Osteoblastic/osteoclastic activity, osteoid tissue formation, development of blood vessels, scaffold degradation, and hard tissue response were evaluated.[24] After the third and eighth weeks of operation, the femur bones were removed for proper sampling and fixed with a 10% formaldehyde solution. Bones were decalcified with a 4% formic acid solution. After decalcification, bones were monitored in Thermo Fisher Scientific Tissue Processor Device's routine night programming. Monitored tissues were blocked in paraffin using a Thermo Histostar device. The obtained paraffin blocks were prepared as 5-micrometer sections using a Leica RM2255 microtome device and then were evaluated under a light microscope after being stained with blue-purple hematoxylin and eosin (H & E) dye.[25] In the obtained images, while hematoxylin dyed bone cells' nuclei and calcium sediments, eosin demonstrates the development of bone cells and tissues by staining the protein content.

TABLE 1 Histological scoring of rat femur regeneration and evaluation of scoring.

Histological parameters		Scores
Osteoblast	Not staining	0
Osteoclast	Too few	1
Osteoid tissue	Mild	2
Blood vessel	Moderate	3
Scaffold degradation	Severe	4

2.5 | Statistical analysis

Statistical analyze performed by using SPSS software version 18. The conformity of the variables to the normal distribution was analyzed using Kolmogorov–Smirnov/Shapiro–Wilk tests. Since the normal distribution was not observed in all groups, the groups were compared using Kruskal-Wallis variance analysis. Comparisons were made using the Mann–Whitney U test and evaluated with the Bonferroni correction.[26] 3 and 8-week results were analyzed with the non-parametric Wilcoxon Test. A statistical significance level of $P < .05$ was considered significant, and evaluations were assessed from statistically significant groups.

3 | RESULTS & DISCUSSION

3.1 | Morphological study of the scaffolds

The microscopic structure of the scaffolds was observed by using SEM photographs (Figure 1). It was seen that all scaffolds have a large, porous, and rough structure. The pore size of the Alg-nHA, Alg-TA-nHA, and Alg-TBC-nHA scaffolds was measured by the Image J program[27] and determined as 65 ± 3, 55 ± 3, and 55 ± 5 µm, respectively. It was seen that TA and TBC slightly decreased the pore size of the scaffolds.

3.2 | Swelling and degradation rate of the scaffolds

The swelling rate (Figure 2A) and degradation rate (Figure 2B) of the scaffolds were determined by the gravimetric method. While the

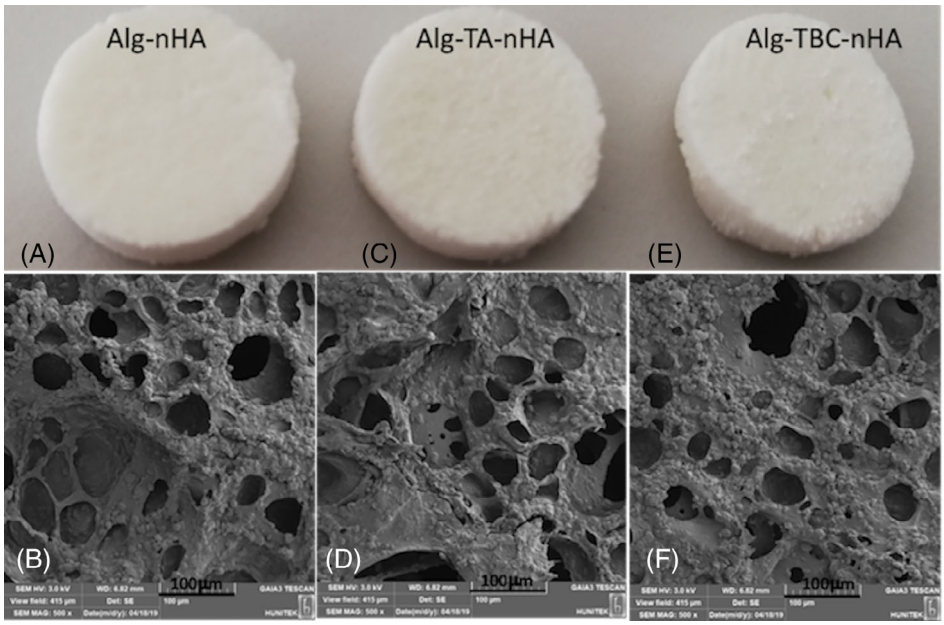

FIGURE 1 Scanning electron microscopy (SEM) and macroscopic photographs of Alg-nHA (A, B), Alg-TA-nHA (C, D) and Alg-TBC-nHA (E, F) scaffolds.

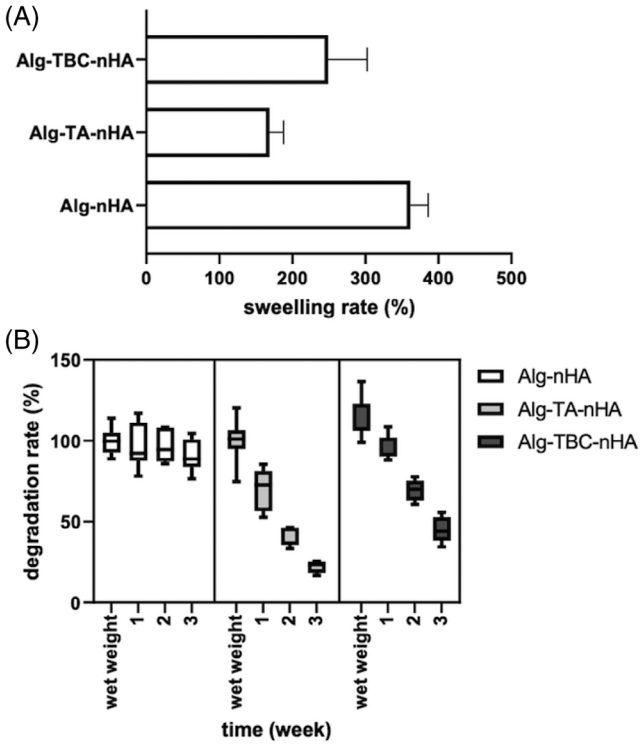

FIGURE 2 Swelling (A) and degradation rate (B) of the scaffolds.

highest swelling rate was observed in Alg-nHA scaffolds ($P < .05$) the lowest swelling rate was observed in Alg-TA-nHA scaffolds (168.7 ± 19.1). TA and TBC modifications were decreased, swelling rate of the scaffolds. Meanwhile, there were observed statistical differences, in the swelling rate of Alg-TA-nHA and Alg-TBC-nHA scaffolds ($P > .05$). At the end of the 1st week, there is no statistical difference in the degradation rate of the scaffolds. However, at the end of the 3rd week, Alg-nHA Alg-TA-nHA and Alg-TBC-nHA mass decreased by an average of 9.3 ± 1.6%, 77.9 ± 3.7%, and 55.7 ± 7.8%, respectively. It was observed that modification of alginate with TA and TBC increased the degradation rate of the scaffolds ($P < .05$). Darabian et al. expressed that TA decreased PLA scaffold degradation.[28] Kurowiak et al. demonstrated that the mass of alginate hydrogels cross-linked with Ca-Ba was about 18%.[29] Forster et al. expressed that in-vivo degradation of the alginate began to be observed after 12 weeks.[30]

3.3 | Chemical characterization of scaffolds

Chemical characterizations of ALG, TA, TBC and modified scaffolds were evaluated by ATR-FTIR. The spectra were presented in Figure 3. At 1421 cm^{-1} the inorganic phosphor group of ALG-nHA was seen.[31] -OH band was seen at 3382 cm^{-1} in the spectrum of ALG-nHA, however, the band was shifted to lower wavenumbers for ALG-TA-nHA at 3276 cm^{-1} and ALG-TBC-nHA at 3254 cm^{-1}.[32] —C═O band of TA was seen at 1738 cm^{-1}, while the —C—O band was observed at 1209 and 1049 cm^{-1}, and the —CO_2 band was seen at 2960 cm^{-1}. For ALG-TA-nHA, the —CO band of TA was shifted to 2944 cm^{-1}. A strong and wide —OH band of ALG-TA-nHA was shifted to 3273 cm^{-1}. The inorganic phosphor of ALG-TA-nHA was seen at, 1415 cm^{-1}. —CH stretching of TBC was seen at 2966, 2935, and 2873 cm^{-1}. —CH deformations of TBC were also seen at 1461 and 1344 cm^{-1}. —C═O band of TBC was seen at 1750 cm^{-1} and the —CO bands were seen at 1181 and 1061 cm^{-1}. For ALG-TBC-nHA, while inorganic phosphor was seen at 1027 cm^{-1}, aliphatic hydrocarbon bands were seen at 2938 cm^{-1}. Besides, a wide —OH peak was seen at 3258 cm^{-1}. Shifting of the bands indicated that there is non-covalent interaction between TA, TBC, and alginate.[33] Interpenetrating polymer fibers can exert blend characteristics during in vivo and in vitro studies.[34]

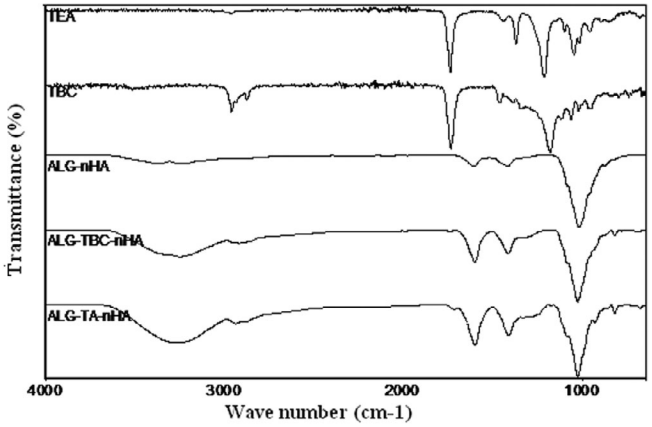

FIGURE 3 Fourier transform infrared spectroscopy – attenuated total reflectance (ATR-FTIR) spectra of TA, TBC, Alg-nHA, Alg-TA-nHA, Alg-TBC-nHA scaffolds.

3.4 | Thermal prosperities of the scaffolds

The thermal properties of the scaffolds were determined by TG (Figure 4A) and DTG (Figure 4B) curves. It was observed that all samples had a gradual loss of weight with an increase in temperature, as shown in TG curves. Around 200°C, there was a sharp decrease in the weight of scaffolds. The decomposition of water, oligomers, TA, and TBC was below 200°C. The plasticization of ALG-nHA with TA and TBC increased the decomposition by approximately 10°C. The DTG curves showed two-weight decrease intervals. Water evaporation was detected below 110°C. Around 200°C, a sharp fragmentation was observed in the samples. Phuong et al. determined the thermal stability of cellulose acetate plasticized with triacetin, diacetin, or phthalate, and they showed that adding plasticizer decreased degradation time.[35] Zhu et al. also used triacetin for starch ester films, and they observed that triacetin decreased the thermal stability of starch film.[36] Darabian et al. reported that mixing TA decreased melting enthalpy of poly lactic acid scaffold.[28]

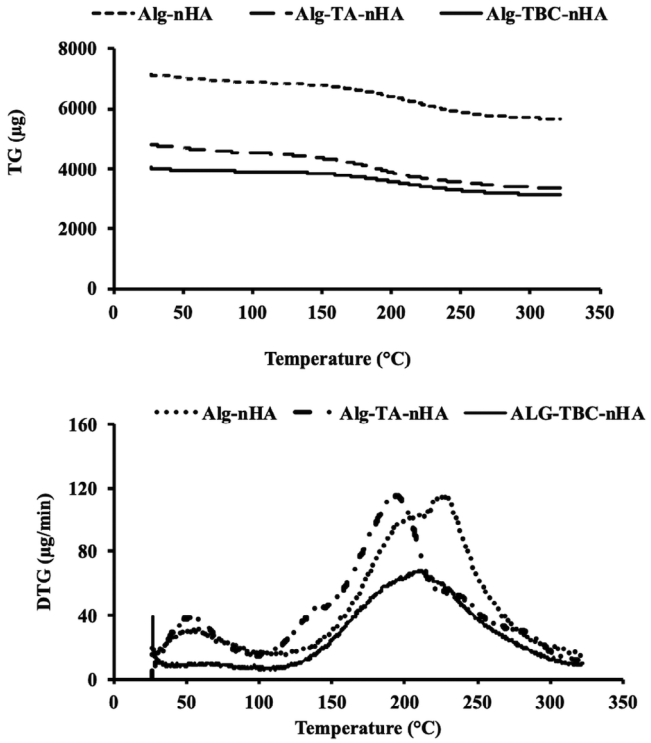

FIGURE 4 TG (A) and DTG (B) curves of Alg-nHA, Alg-TA-nHA, Alg-TBC-nHA scaffolds.

3.5 | Mechanical properties of the scaffolds

The tensile stress and elongation at break values of the scaffolds were determined by the universal mechanical testing machine. ALG-nHA scaffolds have low tensile stress and elongation at the break values found as 8.97 ± 1.8 kPa and 2.00 ± 0.8%, respectively. The tensile stress and elongation at break values of ALG-TBC-nHA scaffolds have been shown to reach 22.22 ± 1.8 kPa and 4.19 ± 1.2%, respectively. However, it was seen that tensile stress and elongation at break of ALG-TA-nHA were 10.08 ± 2.6 kPa and 3.01 ± 1.9%, respectively. In the presented study, the ratio of TBC or TA was 5% (v/v) in alginate scaffolds and the scaffolds were crosslinked with epichlorohydrin. The addition of TA and TBC greatly improved the mechanical properties of alginate scaffolds. Hong-Ru Lin et al. fabricated alginate-HA scaffolds and determined that 50% HA content was optimum for mechanical properties.[37] Yu et al. used acetyl tributyl citrate (ATBC) as the plasticizer and poly (lactic acid) (PLA). They determined that adding ATBC decreased the tensile strength and increased the elongation at the break of their composites.[38] Ghiya et al. also used triethyl citrate and acetyl triethyl citrate as a plasticizer for cellulose acetate. They reported that the addition of triethyl citrate and acetyl triethyl citrate decreased the tensile strength and increased the elongation at the break of cellulose acetate.[39] Our results were compatible with the literature.

3.6 | Cytotoxicity of the scaffolds

Cytotoxicity of the scaffolds on MC-3T3 cells was determined by the MTT test and the results were presented as cell viability, in Figure 5. Accordingly, cytotoxicity of the Alg-nHA, Alg-TA-nHA, and Alg-TBC-nHA scaffold was determined as 3.54 ± 1.38% ($P > .05$), 34.77 ± 7.04% ($P < .05$), 17.2 ± 4.97% ($P < .05$), respectively. It was reported that 2.2 mg/mL concentration of triacetin was cytotoxic on Chinese hamster cells.[40] Meanwhile, Tsen et al. expressed that triacetin did not affect astrocyte cell growth and promoted neural cell expansion.[41] However, it was expressed that a little cytotoxic effect of acetyl tributyl citrate was seen on HeLa cells.[42] Mochida et al. determined LC50 values of acetyl tributyl citrate in some cells as 39.9 ug/mL on Vero cells and 42.1 ug/mL on Madin-Darby canine kidney cells.[43] Our

results demonstrated that the rate of cytotoxicity of TA was more than TBC.

3.7 | Cytokine levels

Over-reaction of the immune response against scaffolds may cause treatment failure. Therefore, IL-1 beta and TNF-alpha expression of the macrophage, which interacted with the scaffold, was determined. Previously, monocyte (THP-1 cells) was differentiated into macrophages, and differentiation was monitored by light microscopy (Figure 6). Macrophages were incubated with scaffolds for 2 days, and cytokines were determined. The levels of IL-1 (Figure 7A) and TNF-alpha (Figure 7B) were presented. According to the results, while Alg-nHA scaffolds did not increase pro-inflammatory cytokines ($P > .05$), Alg-TA-nHA scaffolds increased both IL-1 beta and TNF-alpha levels ($P < .05$). Besides, Alg-TBC-nHA scaffolds increased only TNF-alpha levels ($P < .05$). Cornelia Wiegand et al. demonstrated that alginate sponge reduced pro-inflammatory cytokine levels.[44] Also, Song Yi Seo et al. found similar results concerning alginate sponge.[45]

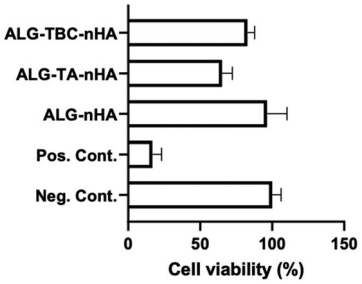

FIGURE 5 Cytotoxicity of the scaffolds on MC-3T3 cells.

3.8 | Histological studies

In-vivo efficiency of the scaffolds was investigated in the drill defect model. A defect of 5 mm dimension was created, and the scaffolds were placed into the defect. 3 and 8 weeks after operations, rat femurs were harvested, and the samples stained with hematoxylin–eosin were examined under a microscope and scored. Osteoblast and osteoid developments were observed significantly

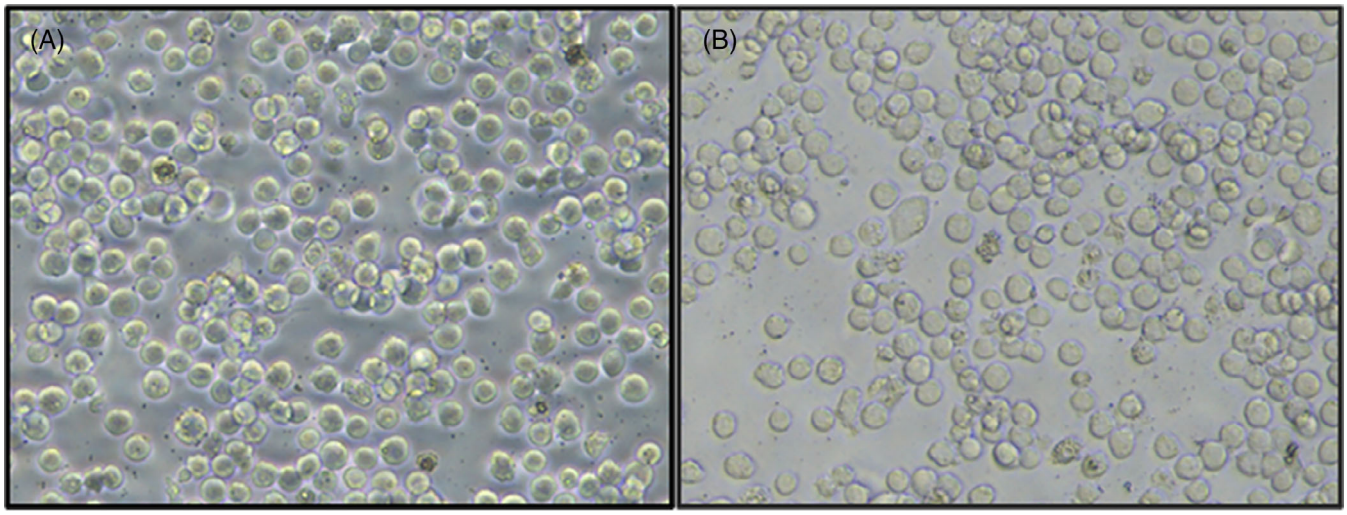

FIGURE 6 THP-1 cells (A) were treated with PMA and transformed into macrophages (B), 20x magnification.

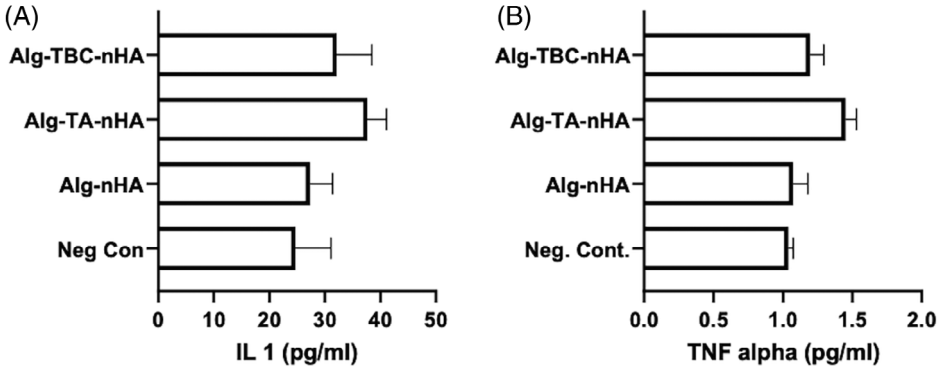

FIGURE 7 IL-1 beta (A) and TNF-alpha (B) expression levels of macrophages, interacted with the scaffolds.

TABLE 2 Mean and STD values of 3 and 8-week experimental groups.

Groups	Histological parameters	Mean	STD	Minimum	Maximum
Alg-nHA	Osteoblast 3th week	2.25	0.463	2	3
	Osteoclast 3th week	1.75	0.463	1	2
	Osteoid tissue 3th week	2	0	2	2
	Blood vessel 3th week	2.25	0.463	2	3
	Scaffold degradation 3th week	3	0	3	3
	Osteoblast 8th week	3.5	0.535	3	4
	Osteoclast 8th week	2	0	2	2
	Osteoid tissue 8th week	2.5	0.535	2	3
	Blood vessel 8th week	2	0	2	2
	Scaffold degradation 8th week	3	0	3	3
Alg-TA-nHA	Osteoblast 3th week	3	0	3	3
	Osteoclast 3th week	2	0	2	2
	Osteoid tissue 3th week	2.5	0.535	2	3
	Blood vessel 3th week	2.5	0.535	2	3
	Scaffold degradation 3th week	3	0	3	3
	Osteoblast 8th week	4	0	4	4
	Osteoclast 8th week	3	0	3	3
	Osteoid tissue 8th week	4	0	4	4
	Blood vessel 8th week	2.5	0.535	2	3
	Scaffold degradation 8th week	4	0	4	4
Alg-TBC-nHA	Osteoblast 3th week	2	0	2	2
	Osteoclast 3th week	2	0	2	2
	Osteoid tissue3th week	1.5	0.535	1	2
	Blood vessel 3th week	1.5	0.535	1	2
	Scaffold degradation 3th week	2	0	2	2
	Osteoblast 8th week	2.5	0.535	2	3
	Osteoclast 8th week	2	0	2	2
	Osteoid tissue 8th week	2.5	0.535	2	3
	Blood vessel 8th week	3	1.069	2	4
	Scaffold degradation 8th week	2.5	0.535	2	3

in the ALG-TA-nHA group 3 weeks after operations, and the scaffolds showed a similar profile of degradation compared to other groups. Likewise, in the 8-week groups, the highest score values were still achieved in the ALG-TA-nHA group, and it seems preferable for use of scaffolds in the other groups (Table 2). Photographs of histological examinations at the end of 3 and 8 weeks are presented in Figure 8. The limitation of this study has not taken a photograph of the control group.

At the end of 3 weeks, while there were no differences in osteoblast development between the Alg-nHA and Alg-TBC-nHA groups, scores of the Alg-TA-nHA group were statistically higher ($P < .05$). Besides, there was no statistically significant difference between the groups in terms of osteoclast scoring ($P > .05$). On the other hand, there were no differences in osteoid tissue scores between Alg-nHA and Alg-TA-nHA groups but, the scores of the Alg-TBC-nHA group were higher than the others ($P < .05$). In terms of blood vascularization scorers, there were no differences between Alg-nHA and Alg-TA-nHA groups, but the scores of the Alg-TBC-nHA group were higher than the others ($P < .05$). There was no difference between Alg-nHA and Alg-TA-nHA groups in terms of degradation scoring of scaffolds ($P > .05$). However, the results of the Alg-TBC-nHA group were higher than the others ($P < .05$). At the end of 8 weeks, while there were no differences in osteoblast development scorers between the Alg-nHA and Alg-TA-nHA groups, scores of the Alg-TBC-nHA group were higher than those of the others ($P < .05$). In terms of osteoclast scoring, there was no difference between Alg-nHA and Alg-TBC-nHA groups, but the results of the Alg-TA-nHA group were higher than the others ($P < .05$). Also, there were no differences in osteoid tissue scores between Alg-nHA and Alg-TBC-nHA groups but, scores of the Alg-TA-nHA group were higher than the others ($P < .05$). In terms of blood vascularization score, there was no statistically significant difference between the groups ($P > .05$). Besides, there was no

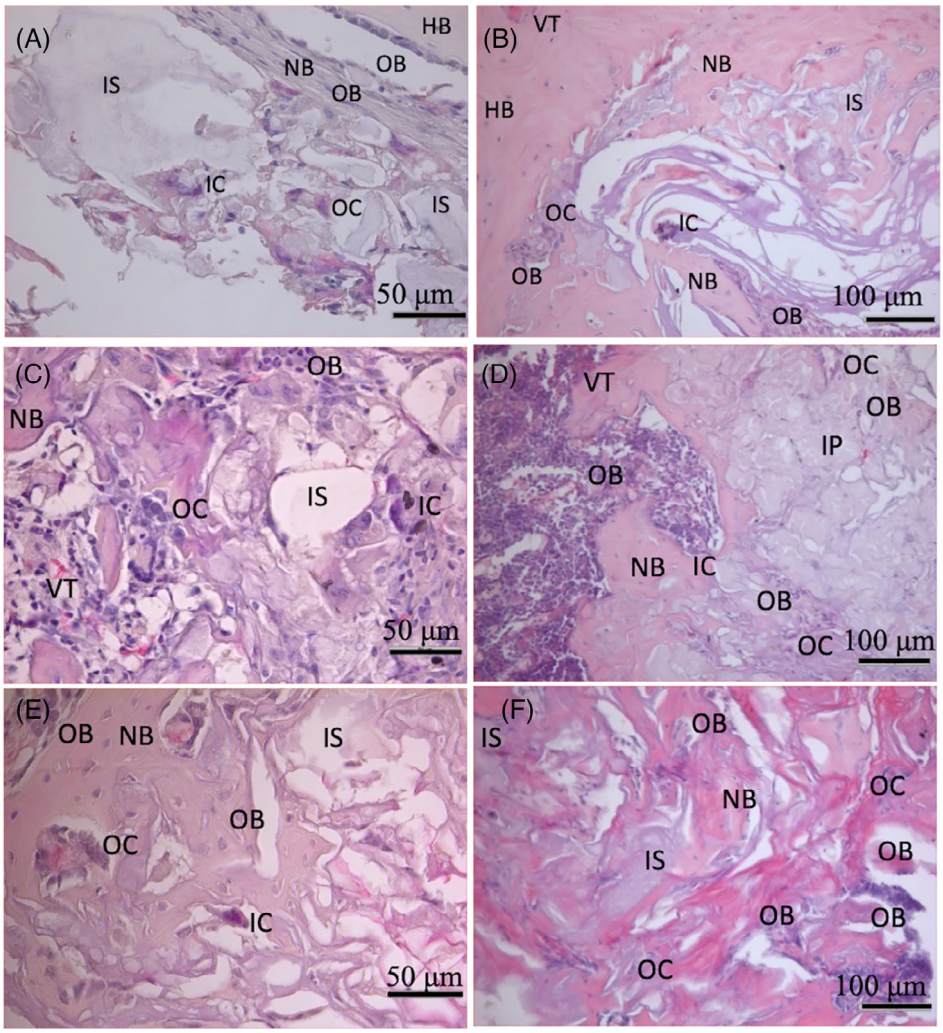

FIGURE 8 Histology photomicrographs of H&E staining of bone defects for three groups after 3 and 8 weeks. Alg-nHA (A, B), Alg-TBC-nHA (C, D), Alg-TA-nHA (E, F). Abbreviations used: host bone (HB), newly bone (NB), vascular tissue (VT), implanted scaffold (IS), inflammatory cell (IC), osteoblast (OB), osteoclast (OC).

difference between the Alg-nHA and Alg-TBC-nHA groups in terms of degradation scoring of scaffolds. But the results of the Alg-TA-nHA group were higher than the others ($P < .05$).

When comparing 3- and 8-week results, osteoblastic development was significant ($P < .05$) in 3 groups, and the most improvement was seen in Alg-nHA and Alg-TA-nHA groups. In terms of osteoclastic development, the change in the Alg-TA-nHA group is seen as statistically significant ($P < .05$). The osteoid tissue development was seen in all groups ($P < .05$), but more growth was in the Alg-TA-nHA group. ALG-TBC-nHA stimulated more neovascularization than other groups ($P < .05$). ALG-TBC-nHA stimulated more neovascularization than other groups ($P < .05$). For degradation scoring, Alg-TA-nHA and Alg-TBC-nHA scaffolds were found to be significant in 8 weeks ($P < .005$). Florczyk et al. fabricated an alginate scaffold containing bone morphogenic protein-2 (BMP-2). They tested the efficiency of the scaffold on a 5 mm in diameter rat drill model and expressed that the scaffold stimulated the reconstruction of critical size defects.[46] Xing et al. fabricated calcium-enriched gellan gum/alginate hydrogel, tested the efficiency of the hydrogel on a 4 mm in diameter rat drill model, and observed that calcium enrichment stimulated neo-vasculature in 8 weeks.[47] Rotten Steiner et al. formed an alginate dialdehyde-gelatin scaffold containing 0.1% nano-bioglass®, expressing the scaffold degradation started after 4-week implantation in-vivo.[48]

4 | CONCLUSION

In this study, alginate scaffolds were plasticized with TA or TBC. According to the FTIR spectra, the shifts in the bands state a non-covalent interaction between TA, TBC, and alginate. It was observed that TBC decreased the thermal stability of the scaffolds, while TA has higher stability. This indicates that TBC does not integrate well between alginate fibers compared to TA, while TA is better integrated and cross-linked with epichlorohydrin. Cell culture studies stated that Alg-TA-nHA was cytotoxic. Alg-TA-nHA and Alg-TBC-nHA increased TNF-alpha levels. Besides, Alg-TA-nHA scaffolds increased IL-1 beta levels. Contrary to cytotoxicity results, in vivo studies indicated that with the addition of TA in a known amount, it is possible to obtain structures that allow both cell invasion and adequate mechanical stability. TBC allowed less cell invasion and bone formation in 8 weeks. It concluded that both modified scaffolds, Alg-TA-nHA and Alg-TBC-nHA increased

bone healing. TA modification leads to more new bone formation than others, and can use as long-term bone treatment.

ACKNOWLEDGMENTS

In-vitro part of the study was conducted at Hacettepe University Advanced Technologies Application and Research Center (HUNITEK) Ankara Turkey.

FUNDING INFORMATION

The study was not supported by any institution or organization.

CONFLICT OF INTEREST STATEMENT

The authors declare that there is no conflict of interest.

DATA AVAILABILITY STATEMENT

Data available on request.

REFERENCES

1. Connelly JT, García AJ, Levenston ME. Inhibition of in vitro chondrogenesis in RGD-modified three-dimensional alginate gels. *Biomaterials*. 2007;28(6):1071-1083.
2. Olivas GI, Barbosa-Cánovas GV. Alginate–calcium films: water vapor permeability and mechanical properties as affected by plasticizer and relative humidity. *LWT-Food Sci Technol*. 2008;41(2):359-366.
3. da Silva MA, Bierhalz ACK, Kieckbusch TG. Alginate and pectin composite films crosslinked with Ca2+ ions: effect of the plasticizer concentration. *Carbohydr Polym*. 2009;77(4):736-742.
4. Córdoba A, Cuéllar N, González M, Medina J. The plasticizing effect of alginate on the thermoplastic starch/glycerin blends. *Carbohydr Polym*. 2008;73(3):409-416.
5. Bialik-Wąs K, Królicka E, Malina D. Impact of the type of crosslinking agents on the properties of modified sodium alginate/poly (vinyl alcohol) hydrogels. *Molecules*. 2021;26(8):2381.
6. Labrecque L, Kumar R, Dave V, Gross R, McCarthy S. Citrate esters as plasticizers for poly (lactic acid). *J Appl Polym Sci*. 1997;66(8):1507-1513.
7. Fiume MM, Heldreth BA, Bergfeld WF, et al. Safety assessment of citric acid, inorganic citrate salts, and alkyl citrate esters as used in cosmetics. *Int J Toxicol*. 2014;33(2):16 S-46 S.
8. Singh S, Maspoch ML, Oksman K. Crystallization of triethyl-citrate-plasticized poly (lactic acid) induced by chitin nanocrystals. *J Appl Polym Sci*. 2019;136(36):47936.
9. Ljungberg N, Andersson T, Wesslén B. Film extrusion and film weldability of poly (lactic acid) plasticized with triacetine and tributyl citrate. *J Appl Polym Sci*. 2003;88(14):3239-3247.
10. Bailey J, Miles JM, Haymond M. Effect of parenteral administration of short-chain triglycerides on leucine metabolism. *Am J Clin Nutr*. 1993;58(6):912-916.
11. Fiume MZ. Final report on the safety assessment of triacetin. *Int J Toxicol*. 2003;22:1-10.
12. Segel R, Anikster Y, Zevin S, et al. A safety trial of high dose glyceryl triacetate for Canavan disease. *Mol Genet Metab*. 2011;103(3):203-206.
13. Liang X, Lin T, Sun G, Beasley-Topliffe L, Cavaillon JM, Warren HS. Hemopexin down-regulates LPS-induced proinflammatory cytokines from macrophages. *J Leukoc Biol*. 2009;86(2):229-235.
14. Lee S-K, Lorenzo J. Cytokines regulating osteoclast formation and function. *Curr Opin Rheumatol*. 2006;18(4):411-418.
15. Gerstenfeld LC, Cho T-J, Kon T, et al. Impaired intramembranous bone formation during bone repair in the absence of tumor necrosis factor-alpha signaling. *Cells Tissues Organs*. 2001;169(3):285-294.
16. Lu Z, Wang G, Dunstan CR, Zreiqat H. Short-term exposure to tumor necrosis factor-alpha enables human osteoblasts to direct adipose tissue-derived mesenchymal stem cells into osteogenic differentiation. *Stem Cells Dev*. 2012;21(13):2420-2429.
17. Lan C, Xiang X, Gao X, Sun D, Pan Y, Li J. Cellular compatibility analysis of nHAp/PPC membrane. *J Hard Tissue Biol*. 2019;28(1):31-36.
18. Shanmugam BK, Rangaraj S, Subramani K, Srinivasan S, Aicher WK, Venkatachalam R. Biomimetic TiO2-chitosan/sodium alginate blended nanocomposite scaffolds for tissue engineering applications. *Mater Sci Eng C*. 2020;110:110710.
19. Khan F, Khanam A, Parihar MS, Bilgainya R, Rai K, Khan F. Dissipative convective structures and nanoparticles encapsulation in Cu/-alginate/dextran composite hydrogels and sponges. *Carbohydr Polym*. 2011;83(2):586-590.
20. El-Aziz A, Asmaa M, El-Maghraby A, Ewald A, Kandil SH. In-vitro cytotoxicity study: cell viability and cell morphology of carbon nanofibrous scaffold/hydroxyapatite nanocomposites. *Molecules*. 2021;26(6):1552.
21. Thomas A, Harding K, Moore K. Alginates from wound dressings activate human macrophages to secrete tumour necrosis factor-α. *Biomaterials*. 2000;21(17):1797-1802.
22. Wu X-Q, Wang D, Liu Y, Zhou J-L. Development of a tibial experimental non-union model in rats. *J Orthopaed Surg Res*. 2021;16(1):1-9.
23. Li Z, Ramay HR, Hauch KD, Xiao D, Zhang M. Chitosan–alginate hybrid scaffolds for bone tissue engineering. *Biomaterials*. 2005;26(18):3919-3928.
24. Liang Y, Zhou R, Liu X, et al. Investigation into the effects of leukemia inhibitory factor on the bone repair capacity of BMSCs-loaded BCP scaffolds in the mouse calvarial bone defect model. *J Bioenerg Biomembr*. 2021;53(4):381-391.
25. Mostafa AA, Mahmoud AA, Hamid MAA, et al. An in vitro/in vivo release test of risedronate drug loaded nano-bioactive glass composite scaffolds. *Int J Pharm*. 2021;607:120989.
26. Tateiwa D, Nakagawa S, Tsukazaki H, et al. A novel BMP-2–loaded hydroxyapatite/beta-tricalcium phosphate microsphere/hydrogel composite for bone regeneration. *Sci Rep*. 2021;11(1):1-13.
27. Chung JJ, Yoo J, Sum BS, et al. 3D printed porous methacrylate/silica hybrid scaffold for bone substitution. *Adv Healthc Mater*. 2021;10(12):2100117.
28. Darabian B, Bagheri H, Mohammadi S. Improvement in mechanical properties and biodegradability of PLA using poly (ethylene glycol) and triacetin for antibacterial wound dressing applications. *Progr Biomater*. 2020;9:45-64.
29. Kurowiak J, Kaczmarek-Pawelska A, Mackiewicz AG, Bedzinski R. Analysis of the degradation process of alginate-based hydrogels in artificial urine for use as a bioresorbable material in the treatment of urethral injuries. *Processes*. 2020;8(3):304.
30. Forster RE, Thürmer F, Wallrapp C, et al. Characterisation of physico-mechanical properties and degradation potential of calcium alginate beads for use in embolisation. *J Mater Sci Mater Med*. 2010;21(7):2243-2251.
31. Kim H-L, Jung G-Y, Yoon J-H, et al. Preparation and characterization of nano-sized hydroxyapatite/alginate/chitosan composite scaffolds for bone tissue engineering. *Mater Sci Eng C*. 2015;54:20-25.
32. Rajkumar M, Meenakshisundaram N, Rajendran V. Development of nanocomposites based on hydroxyapatite/sodium alginate: synthesis and characterisation. *Mater Charact*. 2011;62(5):469-479.
33. Pangesty AI, Todo M. Improvement of mechanical strength of tissue engineering scaffold due to the temperature control of polymer blend solution. *J Funct Biomater*. 2021;12(3):47.
34. Bhati P, Ahuja R, Srivastava A, Singh S, Vashisth P, Bhatnagar N. Physicochemical characterization and mechanical performance analysis of biaxially oriented PLA/PCL tubular scaffolds for intended stent application. *SN Appl Sci*. 2020;2(12):1-11.

35. Phuong VT, Verstiche S, Cinelli P, Anguillesi I, Coltelli M-B, Lazzeri A. Cellulose acetate blends-effect of plasticizers on properties and biodegradability. *J Renew Mater*. 2014;2(1):35-41.
36. Zhu J, Li X, Huang C, Chen L, Li L. Plasticization effect of triacetin on structure and properties of starch ester film. *Carbohydr Polym*. 2013;94(2):874-881.
37. Lin HR, Yeh YJ. Porous alginate/hydroxyapatite composite scaffolds for bone tissue engineering: preparation, characterization, and in vitro studies. *J Biomed Mater Res Part B: Appl Biomater: Off J Soc Biomater Japanese Soc Biomater Austr Soc Biomater Korean Soc Biomater*. 2004;71(1):52-65.
38. Yu J, Wang N, Ma X. Fabrication and characterization of poly (lactic acid)/acetyl tributyl citrate/carbon black as conductive polymer composites. *Biomacromolecules*. 2008;9(3):1050-1057.
39. Ghiya VP, Dave V, Gross RA, Mccarthy SP. Biodegradability of cellulose acetate plasticized with citrate esters. *J Macromolec Sci Part A: Pure Appl Chem*. 1996;33(5):627-638.
40. Abdullah ZW, Dong Y. Recent advances and perspectives on starch nanocomposites for packaging applications. *J Mater Sci*. 2018;53(22):15319-15339.
41. Tsen AR, Long PM, Driscoll HE, et al. Triacetin-based acetate supplementation as a chemotherapeutic adjuvant therapy in glioma. *Int J Cancer*. 2014;134(6):1300-1310.
42. Johnson W Jr. Final report on the safety assessment of acetyl triethyl citrate, acetyl tributyl citrate, acetyl trihexyl citrate, and acetyl trioctyl citrate. *Int J Toxicol*. 2002;21:1-17.
43. Mochida K, Gomyoda M, Fujita T. Acetyl tributyl citrate and dibutyl sebacate inhibit the growth of cultured mammalian cells. *Bull Environ Contam Toxicol*. 1996;56(4):635-637.
44. Wiegand C, Heinze T, Hipler UC. Comparative in vitro study on cytotoxicity, antimicrobial activity, and binding capacity for pathophysiological factors in chronic wounds of alginate and silver-containing alginate. *Wound Repair Regen*. 2009;17(4):511-521.
45. Seo SY, Lee GH, Lee SG, Jung SY, Lim JO, Choi JH. Alginate-based composite sponge containing silver nanoparticles synthesized in situ. *Carbohydr Polym*. 2012;90(1):109-115.
46. Florczyk SJ, Leung M, Li Z, Huang JI, Hopper RA, Zhang M. Evaluation of three-dimensional porous chitosan–alginate scaffolds in rat calvarial defects for bone regeneration applications. *J Biomed Mater Res A*. 2013;101(10):2974-2983.
47. Xing J, Peng X, Li A, et al. Gellan gum/alginate-based Ca-enriched acellular bilayer hydrogel with robust interface bonding for effective osteochondral repair. *Carbohydr Polym*. 2021;270:118382.
48. Rottensteiner U, Sarker B, Heusinger D, et al. In vitro and in vivo biocompatibility of alginate dialdehyde/gelatin hydrogels with and without nanoscaled bioactive glass for bone tissue engineering applications. *Materials*. 2014;7(3):1957-1974.

How to cite this article: Arslan AK, Aydoğdu A, Tolunay T, Basat Ç, Bircan R, Demirbilek M. The effect of alginate scaffolds on bone healing in defects formed with drilling model in rat femur diaphysis. *J Biomed Mater Res*. 2023;111(6):1299-1308. doi:10.1002/jbm.b.35233